Electronic Supplementary Material (ESI) for Journal of Materials Chemistry C.

Electronic Supplementary Information

Hydrogen-bonded organic framework of rigidly branched fluorophore: guest-adaptive cavity and phase-dependent light emission

Hongsik Kim,[a] Hyejin Yoo,[b] Jin Yeong Kim,[b] and Dongwhan Lee[a]*

[a]*Department of Chemistry, Seoul National University, 1 Gwanak-ro, Gwanak-gu, Seoul 08826, Korea*
[b]*Department of Chemistry Education, Seoul National University, 1 Gwanak-ro, Gwanak-gu, Seoul 08826, Korea*

Table of Contents

Experimental Section

1) General Information

General Considerations. All reagents were obtained from commercial suppliers and used as received unless otherwise noted. Toluene used for the synthesis of **TTPE** was saturated with nitrogen and purified by passage through activated Al_2O_3 column under nitrogen (Innovative Technology SPS PureSolv MD4). The compounds **TI**[1] and **TPEBr$_4$**[2] were synthesized according to the reported procedures. All air-sensitive manipulations were carried out under argon atmosphere by standard Schlenk-line techniques. Spectroscopic grade solvents were used for UV–vis and fluorescence measurements.

Physical Measurements. ^{1}H NMR and ^{13}C NMR spectra were recorded on a 500 MHZ Varian/Oxford As-500 spectrometer. Chemical shifts were referenced to the residual solvent peaks.[3] FT-IR spectra were recorded on a PerkinElmer Spectrum Two N FT-NIR Spectrometer. Elemental analysis was performed by a Perkin Elmer 2400 Series II CHNS/O Analyzer. Electronic absorption spectra were recorded on an Agilent 8453 UV–vis spectrophotometer with ChemStation software. Fluorescence spectra were recorded on a Photon Technology International QuantaMaster 400 Spectrofluorometer with FelixGX software (slit size = 2 nm). Quantum yields were determined by using an integrating sphere attached to the instrument (slit size = 1.5 nm). Diffuse reflectance spectra were recorded on a Agilent Cary 5000 UV-Vis-NIR spectrophotometer. The spectral shift of absorption ($\Delta\nu_{\mathrm{abs}}$) were calculated by converting the onset wavelengths (in nm) of the UV–vis absorption (for solution samples) or excitation spectrum (for solid samples) to wavenumbers (in cm^{-1}), and taking difference. Similarly, the spectral shifts of emission ($\Delta\nu_{\mathrm{em}}$) were calculated by converting the maximum intensity wavelengths ($\lambda_{\mathrm{em,max}}$) to wavenumbers, and taking the difference. High-performance liquid chromatography (HPLC) was carried out using a Shimadzu LC-AR system equipped with a normal phase column (CHIRALPAK®, Daicel). Thermogravimetric analysis was carried out with a TA Instruments Q50. Time-resolved photoluminescence (PL) decay measurements were made on an Spectrofluorometer FS5 (Edinburgh) equipped with a 375 nm diode laser (EPL-375). Low-pressure CO_2 and N_2 adsorption–desorption measurements were performed using a Quantachrome Autosorb iQ at 195 K (2-propanol/dry ice bath) and 77 K (liquid nitrogen bath), respectively. Powder XRD patterns were recorded on a Rayonix MX255HS CCD area detector diffractometer using synchrotron radiation (BL2D-SMC at PLSII, λ = 1,20000 Å). Melting points were measured by IA9100 melting point apparatus (Barnstead International).

Gas Sorption Studies. The gas adsorption/desorption isotherms were obtained using a Quantachrome Autosorb iQ. Prior to adsorption measurements, bulk crystal samples of **TTPE** (ca 50 mg) was evacuated ($P < 10^{-5}$ mbar) at r.t. for 3 h.

---

[1] T. Kang, H. Kim and D. Lee, Triazoliptycenes: A twist on iptycene chemistry for regioselective cross-coupling to build nonstacking fluorophores. *Org. Lett.*, 2017, **19**, 6380–6383.

[2] Y. Liu, C. S. Diercks, Y. Ma, H. Lyu, C. Zhu, S. A. Alshmimri, S. Alshihri, O. M. Yaghi, 3D Covalent Organic Frameworks of Interlocking 1D Square Ribbons. *J. Am. Chem. Soc.*, 2019, **141**, 677–683.

[3] G. R. Fulmer, A. J. M. Miller, N. H. Sherden, H. E. Gottlieb, A. Nudelman, B. M. Stoltz, J. E. Bercaw and K. I. Goldberg, NMR chemical shifts of trace impurities: Common laboratory solvents, organics, and gases in deuterated solvents relevant to the organometallic chemist. *Organometallics*, 2010, **29**, 2176–2179.

2) Computations and Simulations

Density Functional Theory (DFT) and Time-Dependent DFT (TD-DFT). All DFT and TD-DFT calculations were carried out using Gaussian 16 suite program[4] (CAM-B3LYP[5]/6-31G(d,p)[6] level of theory). The optimized geometry of **TTPE** was verified by frequency calculations: no imaginary frequencies for the minima.Frontier molecular orbital (FMO) distribution diagrams were generated using the isovalue 0.02

Molecular Electrostatic Potential (MEP) map of TTPE. The MEP map was generated on the crystal structure of **TTPE^{1D}** by using Gaussian 16 suite program[4] (B3LYP[7,8,9]/6-31G(d,p)[6] level of theory).

Simulation of Powder X-Ray Diffraction (PXRD) Pattern. Simulated PXRD patterns were generated with the Mercury software using CIF files obtained without squeezing the solvent molecules (λ = 1.20000 Å).

Hirshfeld Surface of TTPE^{1D} and TTPE^{3D}. Hirshfeld surfaces of solvent-squeezed **TTPE^{1D}** and **TTPE^{3D}** mapped with d_{norm}, and the corresponding fingerprint plots were calculated by using Crystal Explorer 17.5.[10]

[4] M. J. Frisch, G. W. Trucks, H. B. Schlegel, G. E. Scuseria, M. A. Robb, J. R. Cheeseman, G. Scalmani, V. Barone, G. A. Petersson, H. Nakatsuji, X. Li, M. Caricato, A. V. Marenich, J. Bloino, B. G. Janesko, R. Gomperts, B. Mennucci, H. P. Hratchian, J. V. Ortiz, A. F. Izmaylov, J. L. Sonnenberg, D. Williams-Young, F. Ding, F. Lipparini, F. Egidi, J. Goings, B. Peng, A. Petrone, T. Henderson, D. Ranasinghe, V. G. Zakrzewski, J. Gao, N. Rega, G. Zheng, W. Liang, M. Hada, M. Ehara, K. Toyota, R. Fukuda, J. Hasegawa, M. Ishida, T. Nakajima, Y. Honda, O. Kitao, H. Nakai, T. Vreven, K. Throssell, J. A. Montgomery, Jr., J. E. Peralta, F. Ogliaro, M. J. Bearpark, J. J. Heyd, E. N. Brothers, K. N. Kudin, V. N. Staroverov, T. A. Keith, R. Kobayashi, J. Normand, K. Raghavachari, A. P. Rendell, J. C. Burant, S. S. Iyengar, J. Tomasi, M. Cossi, J. M. Millam, M. Klene, C. Adamo, R. Cammi, J. W. Ochterski, R. L. Martin, K. Morokuma, O. Farkas, J. B. Foresman, and D. J. Fox, Gaussian, Inc., Wallingford CT, 2016.

[5] T. Yanai, D. P. Tew, N. C. Handy, A new hybrid exchange–correlation functional using the Coulomb-attenuating method (CAM-B3LYP). *Chem. Phys. Lett.*, 2004, **393**, 51–57.

[6] R. Krishnan, J. S. Binkley, R. Seeger, J. A. Pople, Self-consistent molecular orbital methods. XX. A basis set for correlated wave functions. *J. Chem. Phys.*, 1980, **72**, 650–654.

[7] R. G. Parr, W. Yang, *Density Functional Theory of Atoms and Molecules.* Oxford University Press: New York, 1989.

[8] R. M. Dickson, A. B. Becke, Basis-Set-Free Local Density-Functional Calculations of Geometries of Polyatomic Molecules. *J. Chem. Phys.*, 1993, **99**, 3898–3905.

[9] C. Lee, W. Yang, R. G. Parr, Development of the Colle-Salvetti Correlation-Energy Formula into a Functional of the Electron Density. *Phys. Rev. B.*, 1988, **37**, 785–798.

[10] M. A. Spackman, D. Jayatilaka, Hirshfeld surface analysis. *CrystEngComm*, 2009, **11**, 19–32.

3) Synthetic Procedure

Synthesis and Characterization of TTPE. An oven-dried Schlenk tube was loaded with 1,1,2,2-tetrakis(4-bromophenyl)ethene (**TPE**Br_4, 130 mg, 0.201 mmol), **TI** (248 mg, 1.01 mmol), and potassium phosphate (342 mg, 1.61 mmol) under N_2 atmosphere. To a 4 mL shell vial was added $Pd_2(dba)_3$ (15 mg, 0.016 mmol), $Me_4{}^tBuXPhos$ (25 mg, 0.052 mmol) and dry-toluene (1 mL) under N_2 atmosphere. The catalyst premixture was heated at 120 ℃ for 5 min and cooled to r.t. To the Schlenk tube containing reactants, dry-toluene (5 mL) and catalysis premixture (1 mL) were delivered via syringe. The reaction mixture was heated at 120 °C with stirring for 96 h. After the reaction was completed, the mixture was cooled to r.t., diluted with CH_2Cl_2 (250 mL), and washed with brine (100 mL). The organic fraction was dried over anhydrous $MgSO_4$, filtered, and concentrated under reduced pressure. Flash column chromatography on SiO_2 (CH_2Cl_2 only → CH_2Cl_2/EtOAc = 19:1, v/v) furnished **TTPE** as a white solid (179 mg, 0.137 mmol, yield = 68%). ^{1}H NMR (500 MHz, $CDCl_3$, 298 K): δ 7.56 (d, J = 8.8 Hz, 8H), 7.38 (dt, J = 7.2, 3.6 Hz, 16H), 7.01 (dt, J = 7.2, 3.6 Hz, 16H), 6.98 (d, J = 8.8 Hz ,8H), 5.51 (s, 8H). ^{13}C NMR (125 MHz, $CDCl_3$, 298 K): δ 157.28, 114.90, 141.36, 140.14 139.24, 132.56, 126.23, 124.80, 117.85, 47.03. FT-IR (ATR, cm^{-1}): 3068, 3044, 3019, 2979, 1732, 1604, 1517, 1456, 1418, 1347, 1194, 1178, 1154, 1142, 1103, 938, 913, 837, 804, 787, 743, 632, 621, 510. Anal. Calcd for $C_{90}H_{58.5}N_{12}O_{1.25}$ (**TTPE**·1.25H_2O): C, 81.40; H, 4.44; N, 12.66. Found: C, 81.09; H, 4.52; N, 13.04. m.p. > 400 °C.

4) PXRD Experiments

General Considerations for PXRD Measurements. Synchrotron powder X-ray diffraction data were obtained in transmission mode as Debye–Scherrer pattern with 140 mm sample-to-detector distance and 60 s exposure time on a Rayonix MX225HS CCD area detector with a fixed wavelength ($\lambda = 1.20000$ Å) on BL2D-SMC at Pohang Accelerator Laboratory (PAL) in Korea. The PAL BL2D-SMDC program[11] was used for data collection. The Fit2D program[12] was used for the conversion of integrated two-dimensional (2-D) patterns to one-dimensional (1-D) patterns, wavelength and detector refinement, and the calibration measurement of a National Institute of Standards and Technology (NIST) Si 640c standard samples.

In Situ Variable Pressure PXRD Measurements. Crystal powder samples were packed in a 0.5-mm or 1.0-mm diameter (wall thickness = 0.01 mm) capillary (Hampton Research Inc. glass number 50) in the presence of solvent. In situ variable pressure PXRD measurements were carried out by using a custom-built apparatus equipped with vacuum manifold and goniometer head. Before data collection, sample powder was outgassed at $T = 298$ K under vacuum until the PXRD pattern consistently showed a pure phase. After activation, the sample was cooled to the measurement temperature by using a cryo-stream at $T = 90$ K or 196 K for nitrogen and carbon dioxide, respectively, under vacuum. At each step of variable pressure PXRD measurement, nitrogen gas (ca. 99.9999%) or carbon dioxide gas (ca. 99.9999%) was introduced to the capillary. A fine adjustable needle valve (Swagelok Company) was used to control the pressure from vacuum to 756 torr. At the designated pressure, the sample was allowed to equilibrate for at least 60 seconds prior to recording the diffraction patterns.

Variable Temperature PXRD Measurements. Crystalline samples were packed in a 0.5-mm diameter (wall thickness = 0.01 mm) capillary (Hampton Research Inc. glass number 50) in the presence of the solvent. For variable temperature PXRD measurements, the capillary tube was attached to a custom-made goniometer head with an opening to air and temperature-controlled N_2 stream with a blower equipment (Leister LE MINI Sensor Kit with 5-mm nozzle). The diffraction patterns were measured by varying the temperature from $T = 25$ to 325 °C. At the targeted temperature, the sample was allowed to equilibrate for at least 60 seconds prior to recording the diffraction patterns.

[11] J. W. Shin, K. Eom, D. Moon, BL2D-SMC, The supramolecular crystallography beamline at the Pohang Light Source II, Korea. *J. Synchrotron Rad.*, 2016, **23**. 369–373.

[12] A. P. Hammersley, FIT2D: a multi-purpose data reduction, analysis and visualization program. *J. Appl. Crystallogr.*, 2016, **49**, 646–652.

5) SC-XRD Experiments

X-ray Crystallographic Studies on TTPE^{1D} . Single crystals of **TTPE^{1D}** were obtained by diffusion of *n*-pentane vapor into a chloroform solution of this material at r.t. A colorless needle-shaped crystal (approximate dimensions 0.5 × 0.048 × 0.024 mm^3) was placed onto a nylon loop with Paratone-N oil under cold nitrogen stream at $T = 100$ K. The diffraction data was measured using synchrotron radiation ($\lambda = 0.70000$ Å) employing a PLSII-2D SMC on a Rayonix MX225HS CCD area detector with high precision one-axis goniostat at Pohang Accelerator Laboratory, Korea. The PAL BL2D-SMDC[11] program was used for data collection, and HKL3000sm (Ver.717)[13] was used for cell refinement, reduction, and absorption correction. A total of 12568 reflections were measured (3.982 ° ≤ 2θ ≤ 59.876 °). The structure was solved with the SHELXT[14] structure solution program using intrinsic phasing, and refined with the SHELXL[15] refinement package of OLEX2.[16] The final refinements of **TTPE^{1D}** were performed using the SQUEEZE routine of PLATON package.[17] with the modification of the structural factors for the contribution of the disordered lattice solvent electron densities. A total of 6059 reflections were used in the calculations. The final $R1$ was 0.0728 ($I \geq 2\sigma(I)$) and $wR2$ was 0.2160 (all data). The final $R1$ was 0.0728 ($I \geq 2\sigma(I)$) and $wR2$ was 0.2160 (all data). $C_{90}H_{56}N_{12}{\cdot}2(CHCl_3){\cdot}2(C_5H_{12})$, $M = 1688.49$ g/mol, monoclinic, $C2/c$ (no. 15), $a = 40.931(8)$ Å, $b = 6.3350(13)$ Å, $c = 32.995(7)$ Å, $\beta = 91.29(3)°$, $V = 8553(3)$ Å^3, $Z = 4$, $D_c = 1.311$ g/cm^3. CCDC 2261714 contains the supplementary crystallographic data for this structure.

X-ray Crystallographic Studies on TTPE^{THF} . Single crystals of **TTPE^{THF}** were obtained by diffusion of *n*-pentane vapor into a THF solution of this material at r.t. A colorless needle-shaped crystal (approximate dimensions 0.22 × 0.026 × 0.018 mm^3) was placed onto a nylon loop with Paratone-N oil under cold nitrogen stream at $T = 100$ K. The diffraction data was measured using synchrotron radiation ($\lambda = 0.70000$ Å) employing a PLSII-2D SMC on a Rayonix MX225HS CCD area detector with high precision one-axis goniostat at Pohang Accelerator Laboratory, Korea. The PAL BL2D-SMDC program[11] was used for data collection, and HKL3000sm (Ver.717)[13] was used for cell refinement, reduction, and absorption correction. A total of 13047 reflections were measured (3.166 ° ≤ 2θ ≤ 67.178 °).The structure was solved with the SHELXT[14] structure solution program using intrinsic phasing, and refined with the SHELXL[15] refinement package of OLEX2.[16] The final refinements of **TTPE^{THF}** were performed using the SQUEEZE routine of PLATON package.[17] A total of 9299 unique reflections were used in all calculation. The final $R1$ was 0.0780 ($I \geq 2\sigma(I)$) and $wR2$ was 0.2445 (all data). $C_{90}H_{56}N_{12}{\cdot}1.6(C_4H_8O){\cdot}1.2(C_5H_{12})$, $M = 1507.40$ g/mol, monoclinic, $C2/c$ (no. 15), $a = 40.939(8)$ Å, $b = 6.3270(13)$ Å, $c = 33.007(7)$ Å, $\beta = 91.59(3)°$, $V = 8546(3)$ Å^3, $Z = 4$, $D_c = 1.172$ g/cm^3. CCDC 2261506 contains the supplementary crystallographic data for this structure.

X-ray Crystallographic Studies on TTPE^{3D}. Single crystals of **TTPE^{3D}** were prepared by slow evaporation of acetone solution of **TTPE** over a period of one month. A pale-yellow block-shaped crystal of **TTPE^{3D}** (approximate dimensions 0.056 × 0.030 × 0.028 mm^3) was placed

[13] Z. Otwinowski and W. Minor, Processing of X-ray diffraction data collected in oscillation mode. *Methods Enzymol.*, 1997, **276**, 307–326.

[14] G. M. Sheldrick, SHELXT – Integrated space-group and crystal-structure determination. *Acta Cryst.*, 2015, **A71**, 3–8.

[15] G. M. Sheldrick, Crystal structure refinement with SHELXL. *Acta Cryst.* 2015, **C71**, 3–8.

[16] O. V. Dolomanov, L. J. Bourhis, R. J. Gildea, J. A. K. Howard and H. Puschmann, OLEX2: a complete structure solution, refinment and analysis program. *J. Appl. Cryst.*, 2009, **42**, 339–341.

[17] A. L. Spek, Structural validation in chemical crystallography. *Acta Cryst.*, 2009, **D65**, 148–155.

onto a nylon loop with Paratone-N oil under cold nitrogen stream at $T = 100$ K. The diffraction data was measured using synchrotron radiation ($\lambda = 0.70000$ Å) employing a PLSII-2D SMC on a Rayonix MX225HS CCD area detector with high precision one-axis goniostat at Pohang Accelerator Laboratory, Korea. The PAL BL2D-SMDC[11] program was used for data collection, and HKL3000sm (Ver.717)[13] was used for cell refinement, reduction, and absorption correction. A total of 21111 reflections were measured ($2.808\ ^\circ \leq 2\theta \leq 66.944\ ^\circ$). The structure was solved with the SHELXT[14] structure solution program using intrinsic phasing, and refined with the SHELXL[15] refinement package of OLEX2.[16] The final refinements of **TTPE^{3D}** were performed using the SQUEEZE routine of PLATON package.[16] A total of 11445 unique reflections were used in all calculation. The final $R1$ was 0.0555 ($I \geq 2\sigma(I)$) and $wR2$ was 0.1649 (all data). $C_{90}H_{56}N_{12}{\cdot}3.25(C_3H_6O)$, M = 1494.22 g/mol, monoclinic, $C2/c$ (no. 15), $a = 32.676(7)$ Å, $b = 17.316(4)$ Å, $c = 29.967(6)$ Å, $\beta = 108.09(3)^\circ$, $V = 16118(6)$ Å^3, $Z = 8$, $D_c = 1.232$ g/cm^3. CCDC 2261505 contains the supplementary crystallographic data for this structure.

6) Validation Reply Form

Validation Reply Form: Detailing any alerts in the **TTPE^{THF}** crystal structure.
_vrf_PLAT029_ALERT_3_A
Problem: _diffrn_measured_fraction_theta_full value Low 0.894
Response: The low completeness was inevitable because of the small needle-shaped crystal of **TTPE^{THF}** (approximate dimensions 0.22 × 0.026 × 0.018 mm^3) and diffraction measurement method (omega scan).

7) Supplementary Tables

Table S1. Hydrogen bonds in **TTPE^{1D}**.

D–H···A	d(D–H)	d(H···A)	d(D···A)	∠DHA
C(00J)–H(00J)···N(003)	0.98	2.44	3.389(3)	164
C(19)–H(19)···N(3)	0.94	2.5	3.469(3)	171

Symmetry transformations used to generate equivalent atoms:
#1 x, –1+y, z #2 x, 1+y, z

Table S2. Summary of X-ray crystallographic data.

	TTPE^{1D}	**TTPE^{THF}**	**TTPE^{3D}**
Crystal system	monoclinic	monoclinic	monoclinic
Space group	$C2/c$	$C2/c$	$C2/c$
Color of crystal	colorless	colorless	pale yellow
a (Å)	40.931(8)	40.939(8)	32.676(7)
b (Å)	6.3350(13)	6.3270(13)	17.316(4)
c (Å)	32.995(7)	33.007(7)	29.967(6)
β (°)	91.29(3)	91.59(3)	108.09(3)
Cell volume (Å^3)	8553(3)	8546(3)	16118(7)
Z	4	4	8
R_{int}	0.0590	0.0254	0.0381

Table S3. Calculated energy levels of FMOs.

	TTPE	**TTPE^{1D}** monomer	**TTPE^{1D}** dimer[a]
HOMO	-0.26 eV	0.07 eV	0.10 / 0.10 eV
LUMO	-6.18 eV	-6.50 eV	-6.45 / -6.45 eV

[a]The **TTPE^{1D}** dimer has degenerate HOMOs and LUMOs.

8) Supplementary Figures

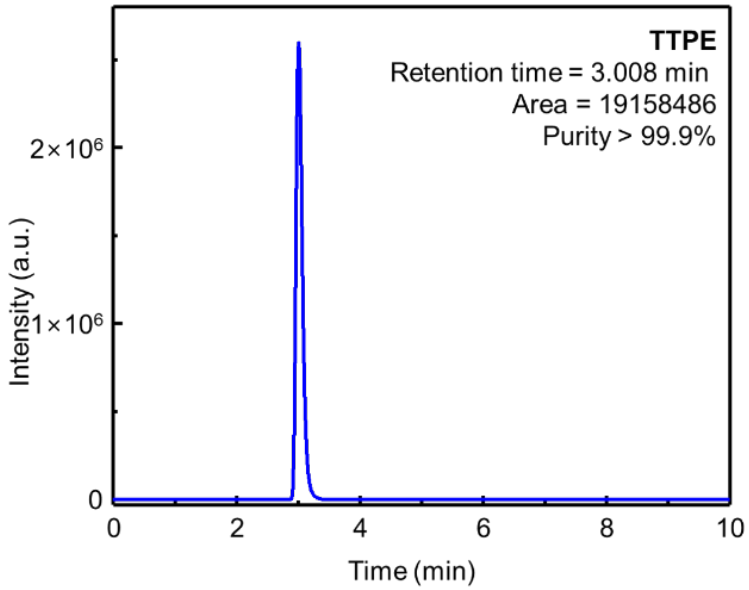

Fig. S1. HPLC chromatogram of **TTPE** (eluent = $CHCl_3$/EtOH/Hexane = 8:1:1, v/v/v).

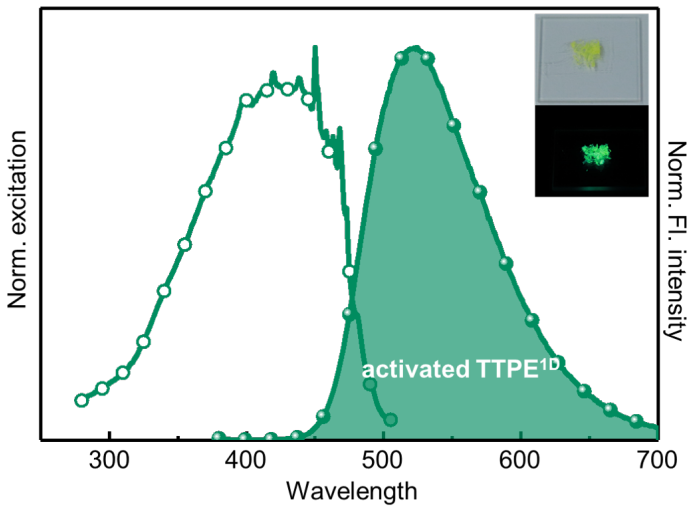

Fig. S2. Normalized solid-state excitation (empty circles) and fluorescence (filled circles) spectra (T = 293 K) of activated $\mathbf{TTPE^{1D}}$. Emission spectra were obtained with λ_{exc} = 370 nm; excitation spectra were recorded for the maximum emission wavelength. Insets are photographic images of the samples under daylight (top) and under UV-lamp (λ = 365 nm, bottom).

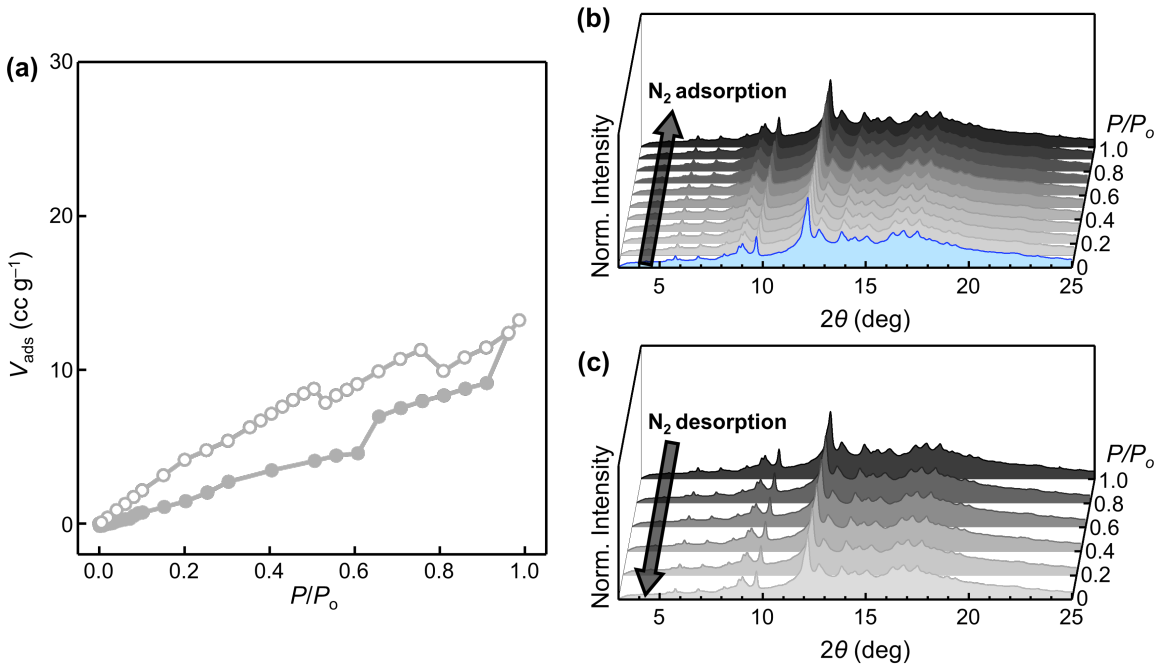

Fig. S3. (a) N_2 adsorption (filled circles) and desorption (empty circles) isotherms of **activated TTPE^{1D}** (T = 77 K). (b, c) PXRD pattern changes recorded during (b) adsorption and (c) desorption of N_2 (T = 90 K).

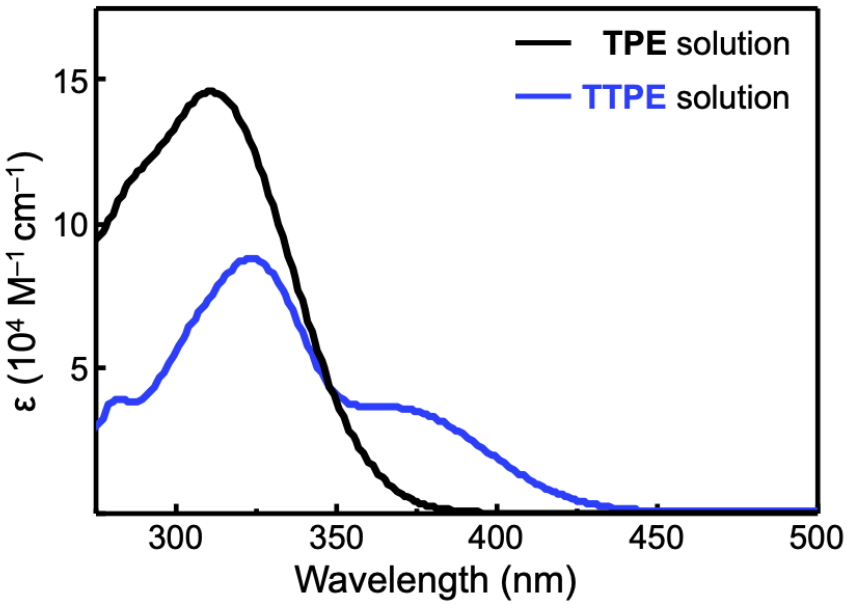

Fig. S4. UV–vis absorption spectra of **TTPE** (blue) and **TPE** (black) in $CHCl_3$ (T = 293 K).

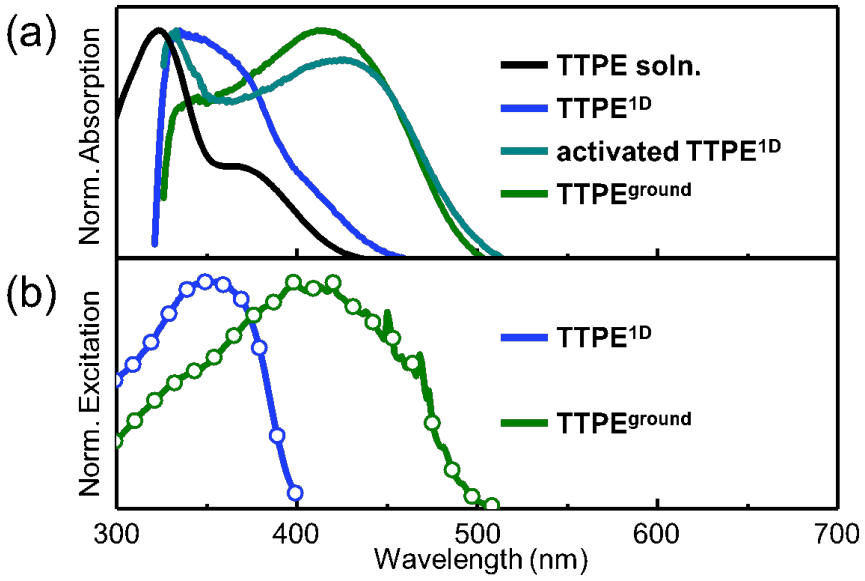

Fig. S5.(a) Normalized UV–vis absorption spectrum of **TTPE** (10 μM in $CHCl_3$) and diffuse reflectance spectra of $\mathbf{TTPE^{1D}}$, activated $\mathbf{TTPE^{1D}}$, and $\mathbf{TTPE^{ground}}$. (b) Normalized excitation spectra of $\mathbf{TTPE^{1D}}$ and $\mathbf{TTPE^{ground}}$ recorded at $\lambda_{em,max}$.

(a)

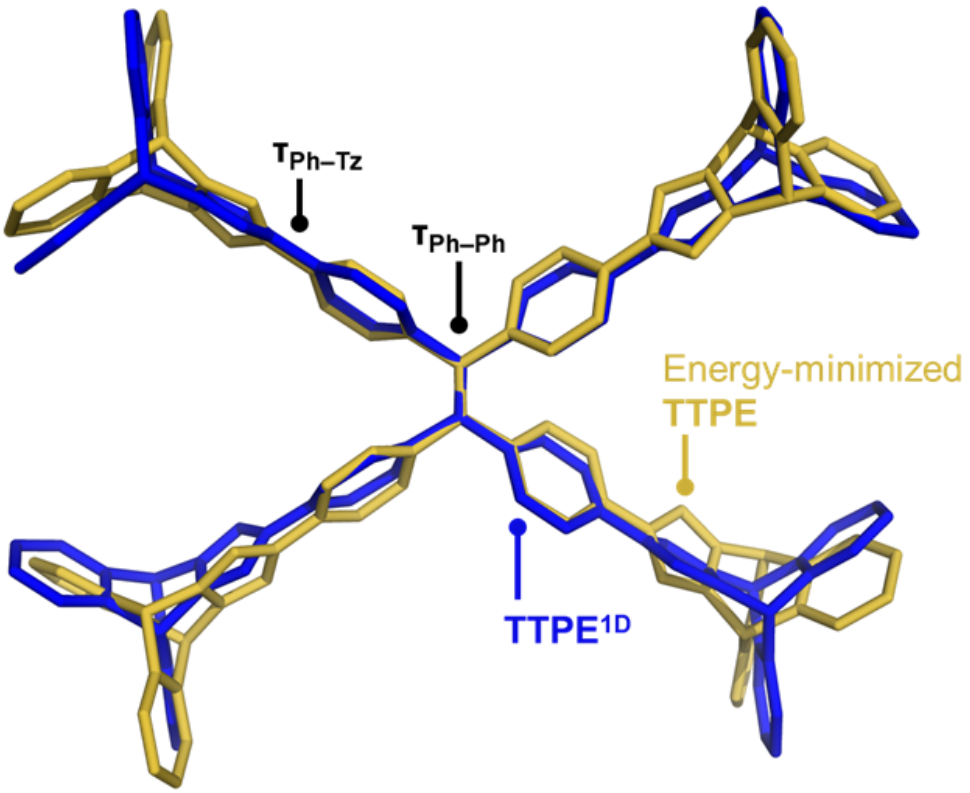

(b)

	$T_{Ph–Ph, avg.}$	$T_{Ph–Tz, avg.}$
TTPE	76.05	0.52
$TTPE^{1D}$	84.78	28.12

Fig. S6. (a) Overlaid capped-stick representations of DFT energy-minimized structure (yellow) and X-ray structure (**$TTPE^{1D}$**, blue) of **TTPE**. Hydrogen atoms were omitted for clarity. (b) A summary of key metric parameters. The twist angles were determined using the normal vectors of the mean-planes.

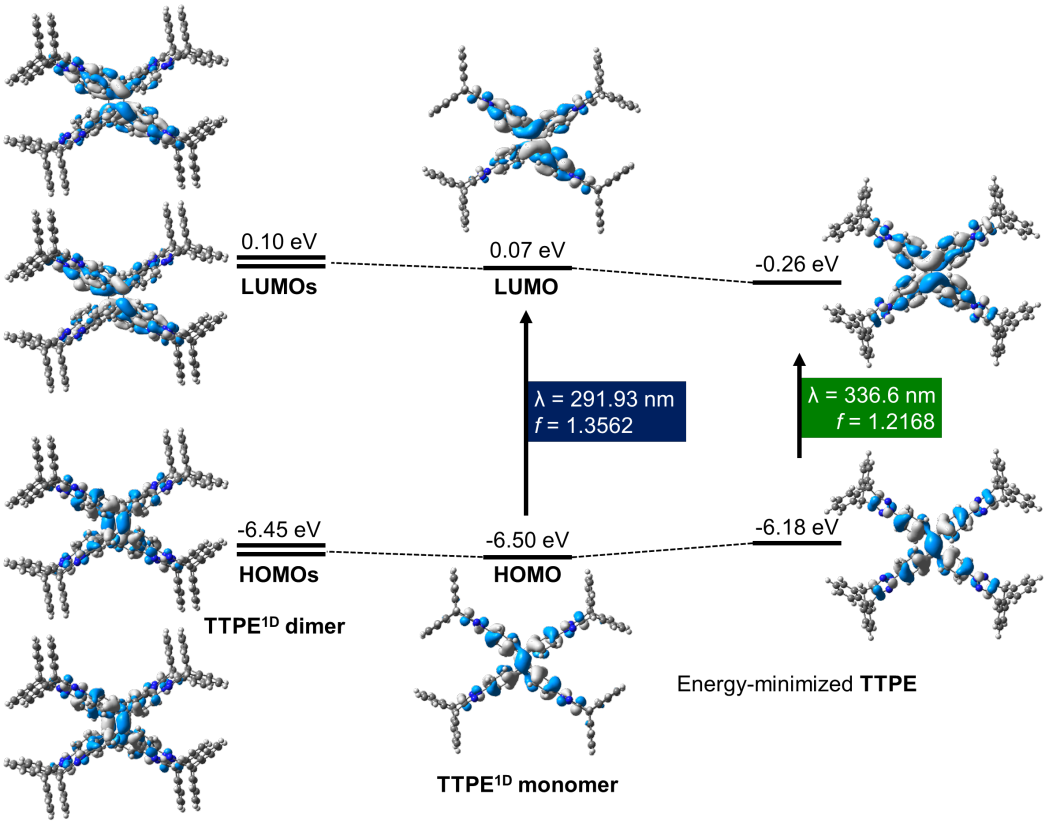

Fig. S7. Changes in the FMO energy levels of **TTPE** in the fully relaxed conformation (right) and within the crystal lattice of **TTPE^{1D}** as monomeric (middle) and dimeric (left) forms. The wavelengths and oscillator strengths (f) of HOMO-to-LUMO electronic transitions, leading to the lowest-energy excited states, were calculated using TD-DFT (CAM-B3LYP/6-31G(d,p) level of theory).

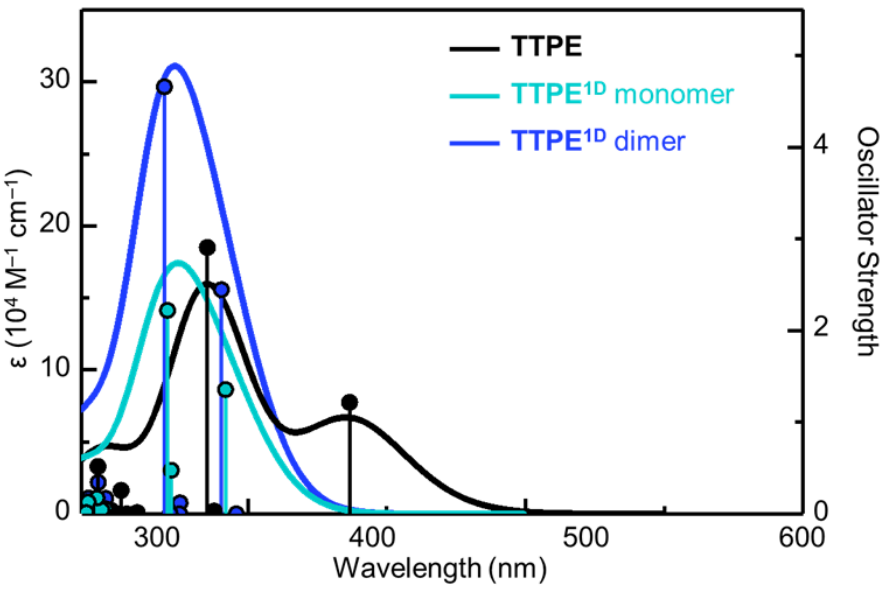

Fig. S8. TD-DFT (CAM-B3LYP/6-31G(d,p) level of theory) computed UV–vis absorption spectra of energy-minimized **TTPE** (black line), **TTPE^{1D}** monomer (cyan line), and **TTPE^{1D}** dimer (blue line), and the corresponding electronic transitions (shown as scatter charts with drop lines).

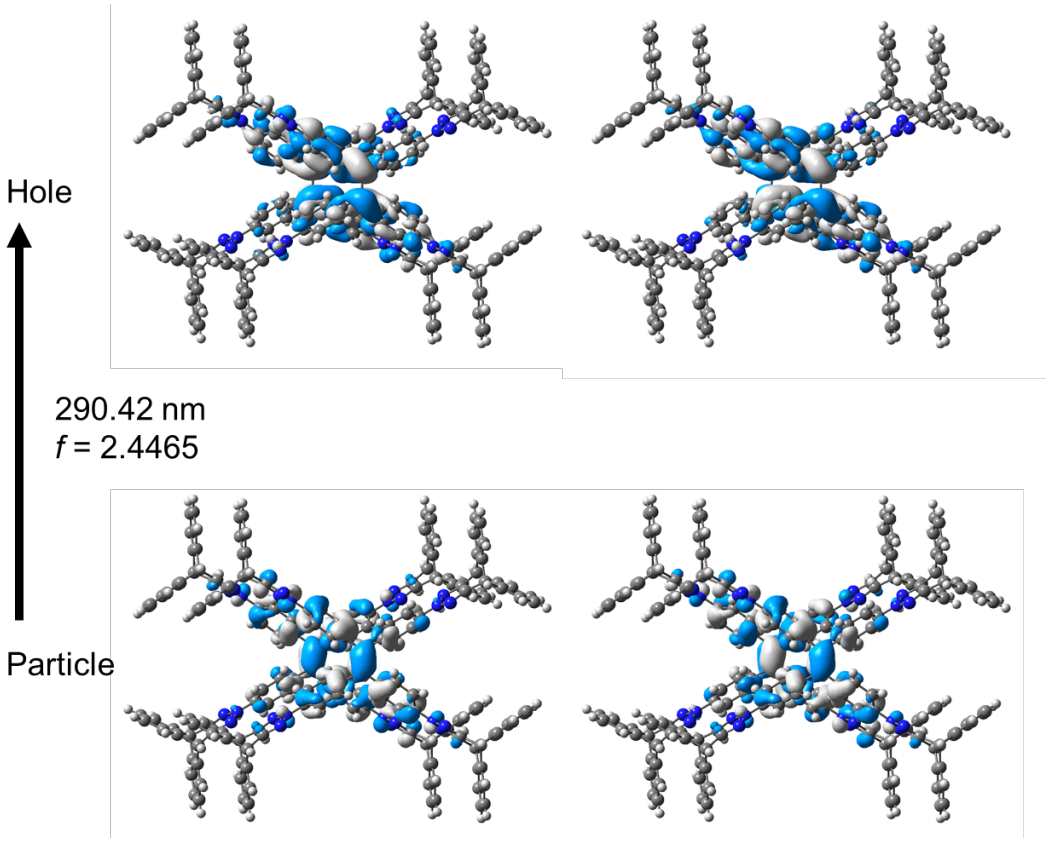

Fig. S9. Natural transition orbitals (NTOs) analysis of $\mathbf{TTPE^{1D}}$ dimer.

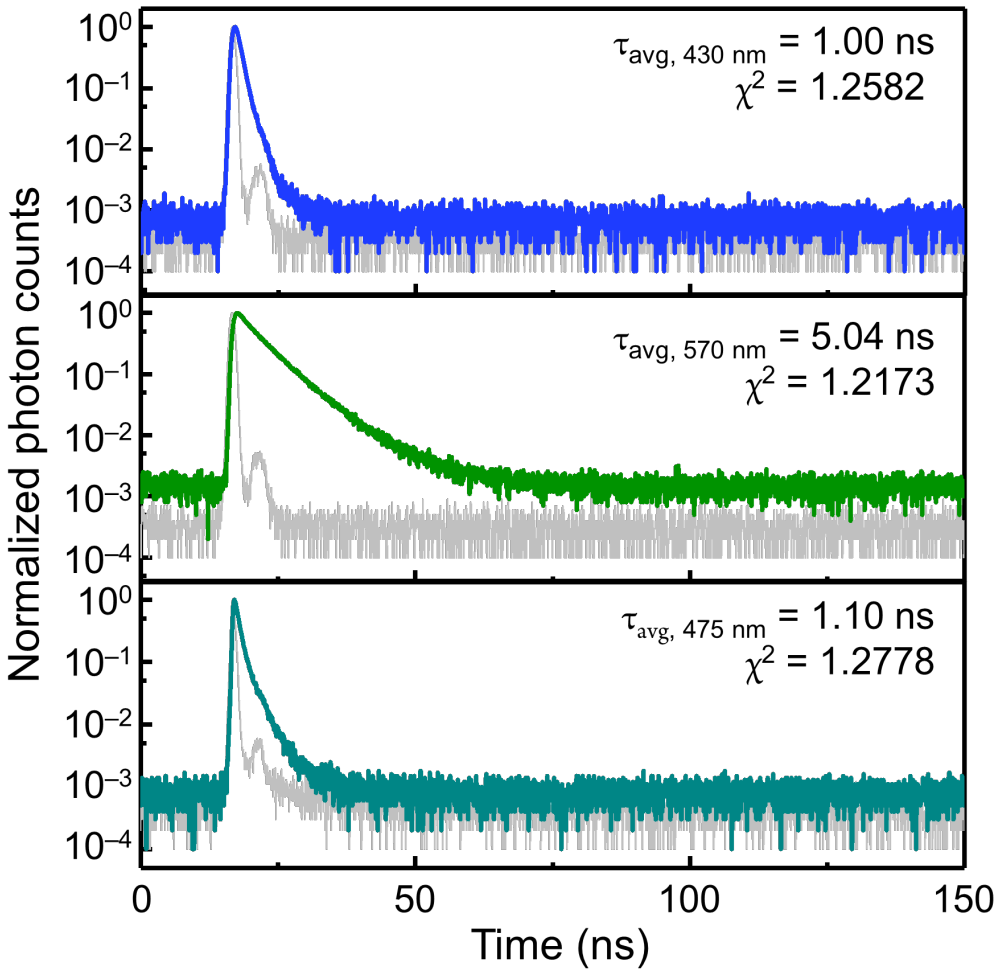

Fig. S10. Transient photoluminescence spectra of $\mathbf{TTPE^{1D}}$ (top), $\mathbf{TTPE^{ground}}$ (middle), and $\mathbf{TTPE^{3D}}$ (bottom) measured at $T = 298$ K.

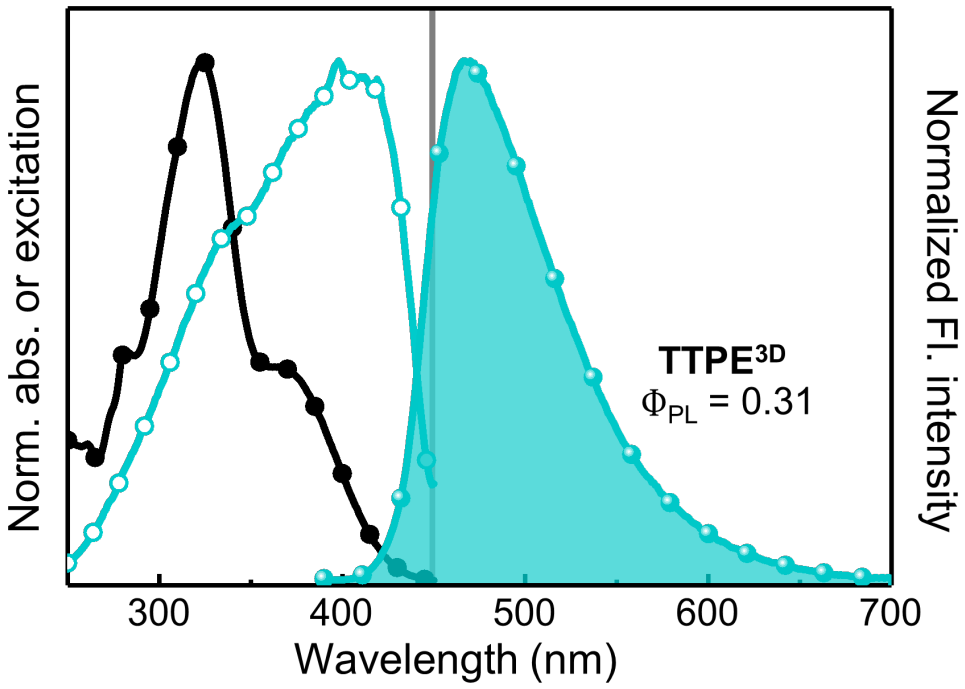

Fig. S11. Photophysical properties of **TTPE^{3D}**. Normalized UV–vis absorption (black filled circles) in $CHCl_3$, solid-state excitation (cyan empty circles), and fluorescence (cyan filled circles) spectra of **TTPE^{3D}**. Emission spectra were recorded with $\lambda_{exc} = 370$ nm; excitation spectra were recorded for the maximum emission wavelength ($T = 293$ K).

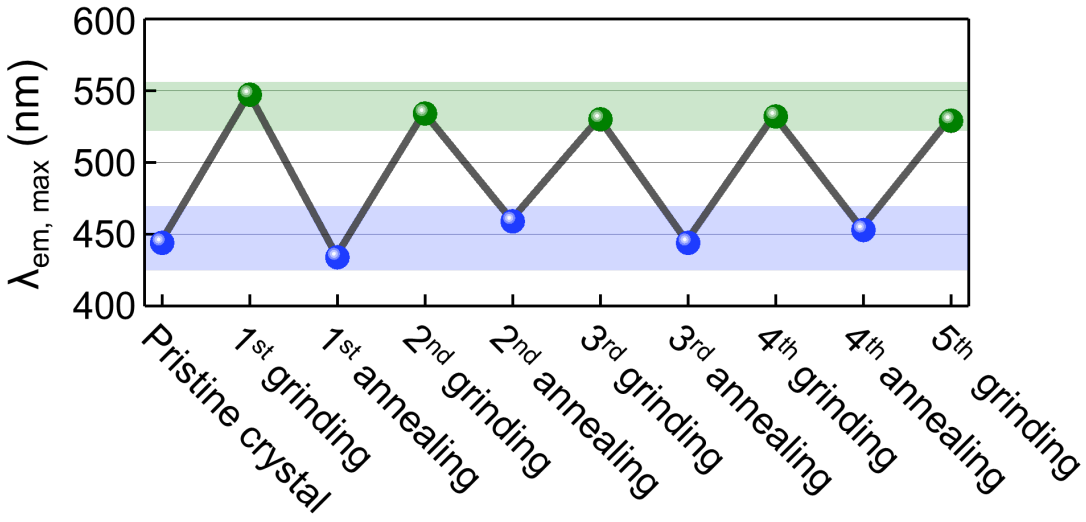

Fig. S12. Changes in the maximum emission wavelength ($\lambda_{\mathrm{em,\ max}}$) monitored during the five-repeated cycles of grinding-and-annealing.

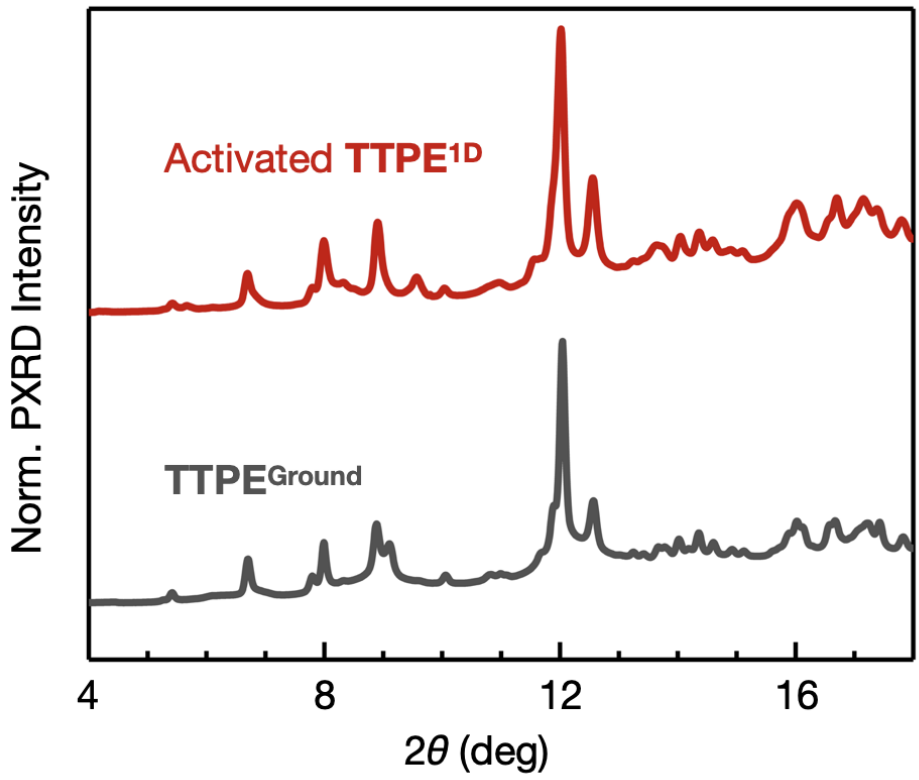

Fig. S13. PXRD patterns of **activated TTPE^{1D}** (top), and **TTPE^{ground}** (bottom) at $T = 298$ K.

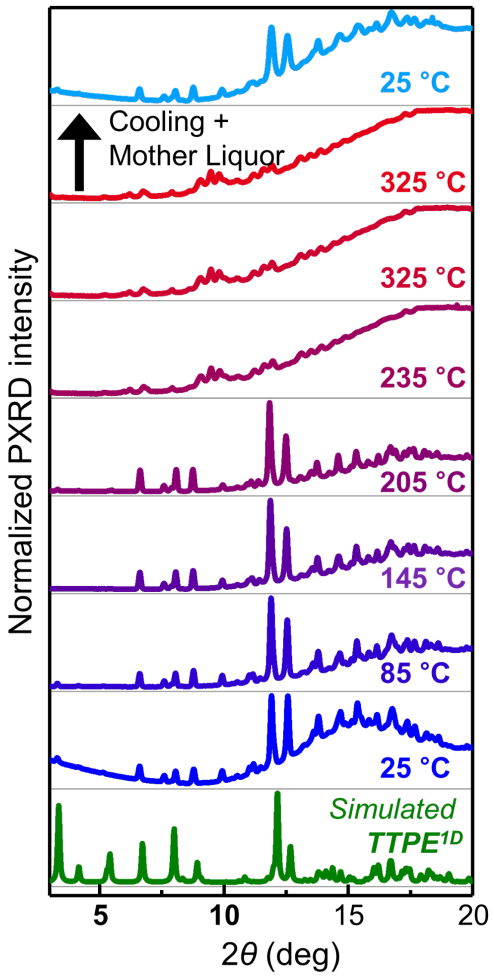

Fig. S14. PXRD patterns of $\mathbf{TTPE^{1D}}$ recorded at various temperatures.

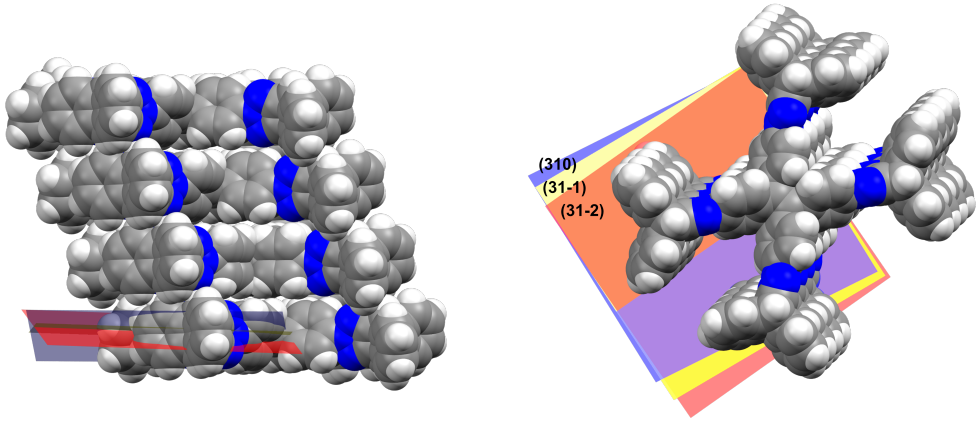

Fig. S15. The (310), (31-1), and (31-2) planes of **TTPE^{1D}** bisecting the **TTPE** molecule in a direction orthogonal to the 1D-assembly viewed from different perspectives.

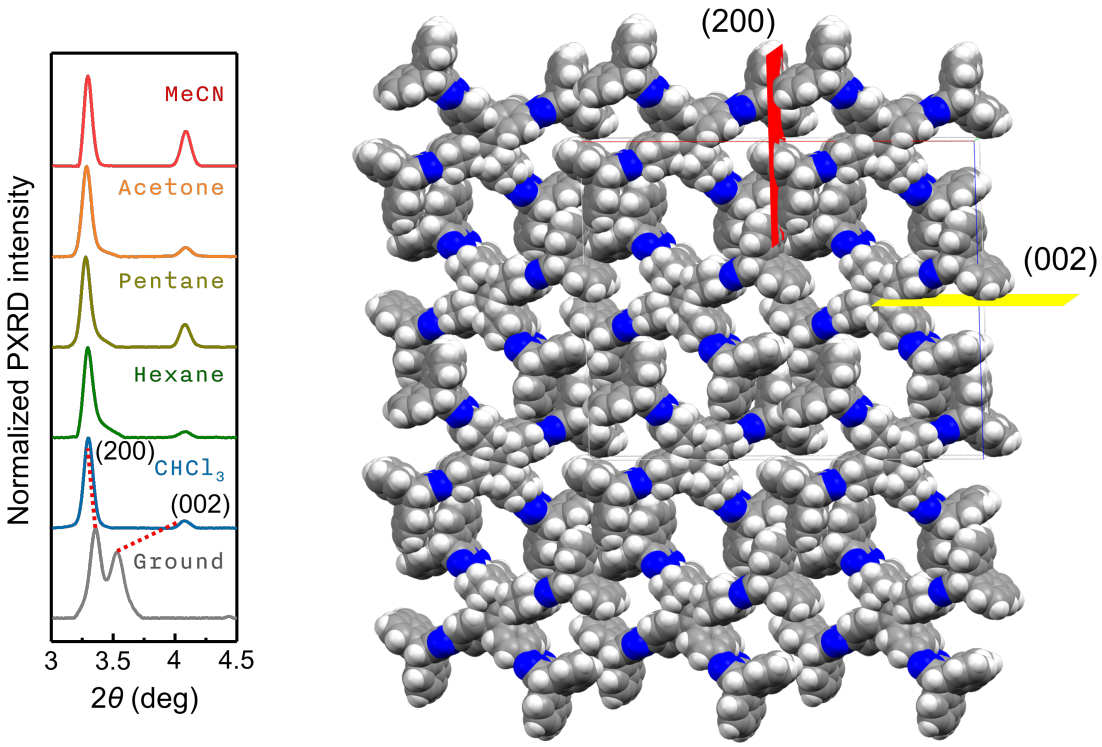

Fig. S16. Magnified PXRD patterns showing the (200) and (002) peaks (left), and the corresponding planes overlaid in the space-filling model (right).

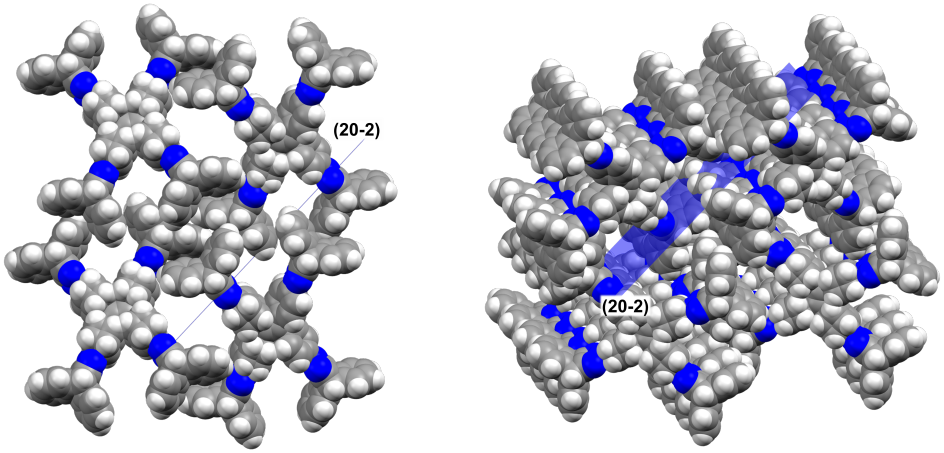

Fig. S17. The (20-2) plane of $\mathbf{TTPE^{1D}}$, bisecting the pores viewed from different perspectives.

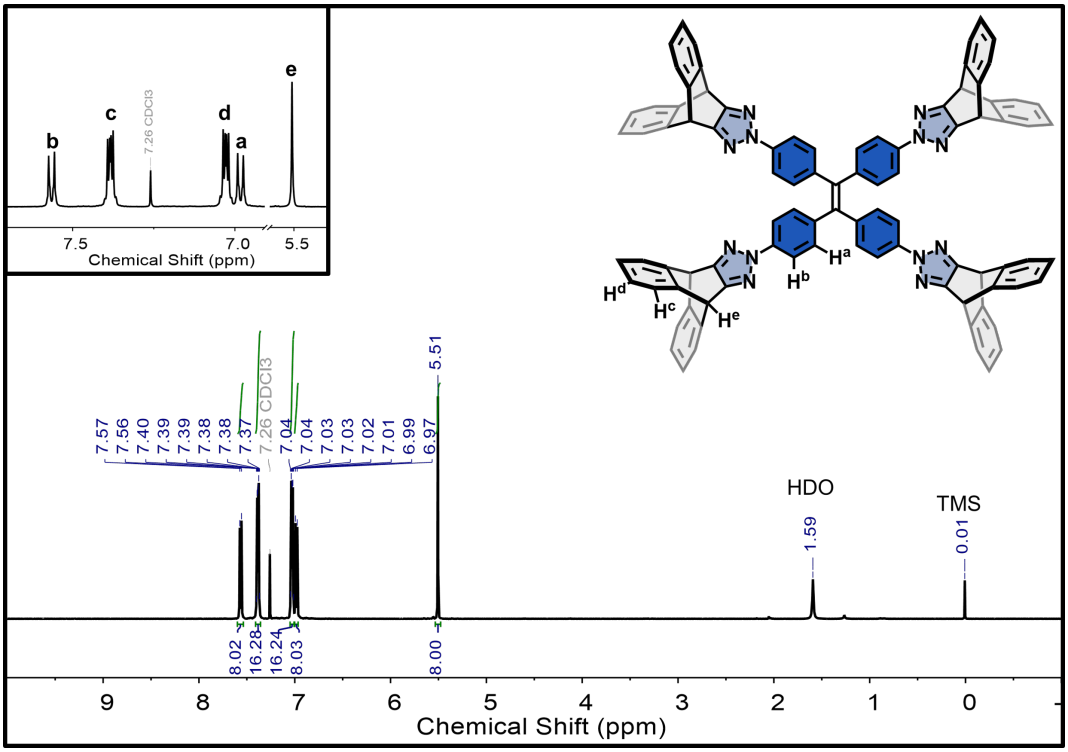

Fig. S18. ^{1}H NMR (500 MHz) spectrum of **TTPE** in $CDCl_3$ (T = 298 K).

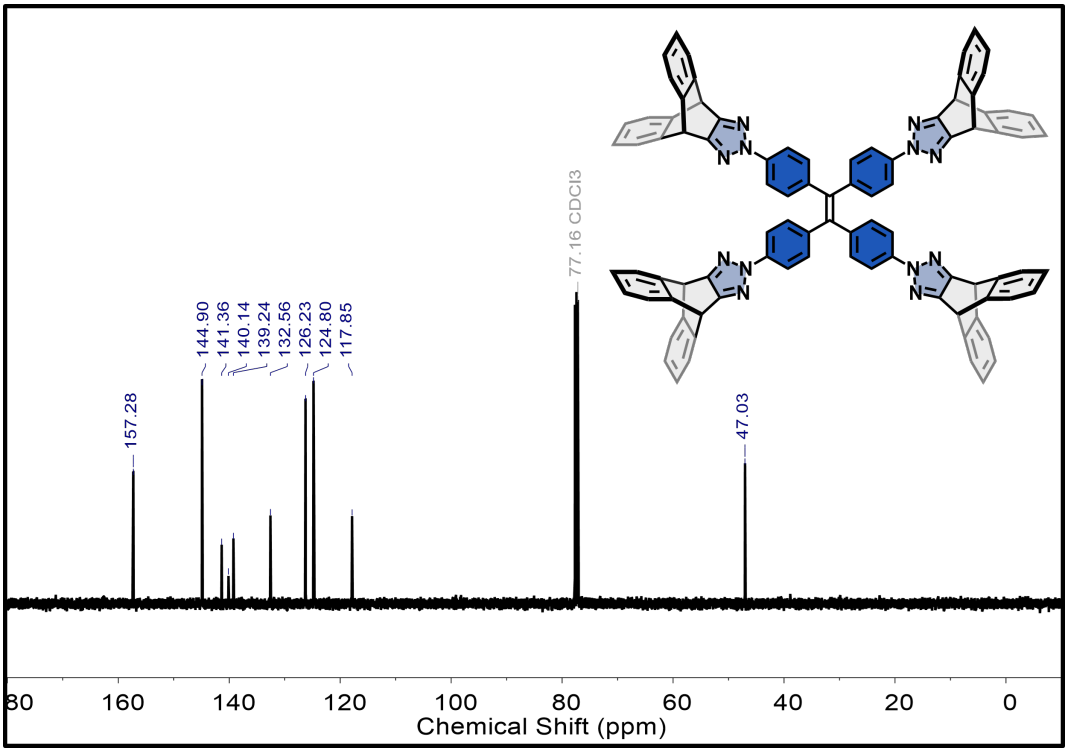

Fig. S19. ^{13}C NMR (125 MHz) spectrum of **TTPE** in $CDCl_3$ (T = 298 K).

Cartesian coordinates of energy-minimized model of **TTPE**,
E(CAM-B3LYP) = –4118.06206727 Hartree.

C	3.33379	-1.99703	-1.25588	C	-7.63060	8.42604	-3.52959
C	1.48685	-2.56134	0.73748	C	-7.03643	8.58988	-1.19588
C	3.55393	-3.04916	-0.37229	C	-7.64828	6.45869	-2.15438
C	2.18921	-1.22741	-1.12377	C	-7.84144	7.05316	-3.38744
C	1.24880	-1.48380	-0.12182	C	-7.23114	9.18857	-2.44212
C	2.63050	-3.33587	0.62863	C	-8.83403	4.94999	-0.66097
C	0.00000	-0.67801	0.00000	C	-10.44020	5.10716	1.59834
C	0.00000	0.67801	0.00000	C	-8.42988	5.72192	0.43971
C	-1.24880	-1.48380	0.12182	C	-10.03376	4.26401	-0.62656
C	-3.55393	-3.04916	0.37229	C	-10.83942	4.34441	0.51092
C	-2.18921	-1.22741	1.12377	C	-9.22912	5.80111	1.56491
C	-1.48685	-2.56134	-0.73748	C	-8.83403	-4.94999	0.66097
C	-2.63050	-3.33587	-0.62863	C	-10.44020	-5.10716	-1.59834
C	-3.33379	-1.99703	1.25588	C	-10.03376	-4.26401	0.62656
C	1.24880	1.48380	0.12182	C	-8.42988	-5.72192	-0.43971
C	3.55393	3.04916	0.37229	C	-9.22912	-5.80111	-1.56491
C	1.48685	2.56134	-0.73748	C	-10.83942	-4.34441	-0.51092
C	2.18921	1.22741	1.12377	C	-7.24397	-7.23053	1.05367
C	3.33379	1.99703	1.25588	C	-7.63060	-8.42604	3.52959
C	2.63050	3.33587	-0.62863	C	-7.64828	-6.45869	2.15438
C	-1.24880	1.48380	-0.12182	C	-7.03643	-8.58988	1.19588
C	-3.55393	3.04916	-0.37229	C	-7.23114	-9.18857	2.44212
C	-1.48685	2.56134	0.73748	C	-7.84144	-7.05316	3.38744
C	-2.18921	1.22741	-1.12377	H	4.05675	-1.79632	-2.03556
C	-3.33379	1.99703	-1.25588	H	0.76132	-2.79609	1.50919
C	-2.63050	3.33587	0.62863	H	2.02055	-0.40780	-1.81291
N	4.72021	3.83939	0.49802	H	2.81562	-4.16130	1.30340
N	5.63897	3.61641	1.45268	H	-2.02055	-0.40780	1.81291
C	6.53604	4.54861	1.22165	H	-0.76132	-2.79609	-1.50919
C	6.13267	5.31878	0.12305	H	-2.81562	-4.16130	-1.30340
N	4.98494	4.86509	-0.32874	H	-4.05675	-1.79632	2.03556
N	-4.72021	3.83939	-0.49802	H	0.76132	2.79609	-1.50919
N	-5.63897	3.61641	-1.45268	H	2.02055	0.40780	1.81291
C	-6.53604	4.54861	-1.22165	H	4.05675	1.79632	2.03556
C	-6.13267	5.31878	-0.12305	H	2.81562	4.16130	-1.30340
N	-4.98494	4.86509	0.32874	H	-0.76132	2.79609	1.50919
N	-4.72021	-3.83939	0.49802	H	-2.02055	0.40780	-1.81291
N	-4.98494	-4.86509	-0.32874	H	-4.05675	1.79632	-2.03556
C	-6.13267	-5.31878	0.12305	H	-2.81562	4.16130	1.30340
C	-6.53604	-4.54861	1.22165	H	-6.77975	-7.03238	-1.09437
N	-5.63897	-3.61641	1.45268	H	-8.16811	-4.38114	2.68624
N	4.72021	-3.83939	-0.49802	H	-8.16811	4.38114	-2.68624
N	4.98494	-4.86509	0.32874	H	-6.77975	7.03238	1.09437
C	6.13267	-5.31878	-0.12305	H	8.16811	4.38114	2.68624
C	6.53604	-4.54861	-1.22165	H	6.77975	7.03238	-1.09437
N	5.63897	-3.61641	-1.45268	H	6.77975	-7.03238	1.09437
C	-7.08430	-6.42690	-0.24091	H	8.16811	-4.38114	-2.68624
C	-7.84511	-4.97418	1.83084	H	7.06777	-10.25497	-2.55793
C	-7.84511	4.97418	-1.83084	H	8.15342	-6.45565	-4.23876
C	-7.08430	6.42690	0.24091	H	6.72292	-9.18637	-0.34442

C	7.84511	4.97418	1.83084	H	7.77977	-8.89587	-4.49619
C	7.08430	6.42690	-0.24091	H	11.78111	-3.80628	0.54213
C	7.08430	-6.42690	0.24091	H	8.91577	-6.39774	2.41633
C	7.84511	-4.97418	-1.83084	H	11.06953	-5.16583	2.48028
C	7.64828	-6.45869	-2.15438	H	10.34543	-3.66614	-1.47771
C	7.23114	-9.18857	-2.44212	H	11.78111	3.80628	-0.54213
C	7.84144	-7.05316	-3.38744	H	8.91577	6.39774	-2.41633
C	7.24397	-7.23053	-1.05367	H	10.34543	3.66614	1.47771
C	7.03643	-8.58988	-1.19588	H	11.06953	5.16583	-2.48028
C	7.63060	-8.42604	-3.52959	H	7.06777	10.25497	2.55793
C	8.42988	-5.72192	0.43971	H	8.15342	6.45565	4.23876
C	10.83942	-4.34441	0.51092	H	7.77977	8.89587	4.49619
C	8.83403	-4.94999	-0.66097	H	6.72292	9.18637	0.34442
C	9.22912	-5.80111	1.56491	H	-7.77977	8.89587	-4.49619
C	10.44020	-5.10716	1.59834	H	-6.72292	9.18637	-0.34442
C	10.03376	-4.26401	-0.62656	H	-8.15342	6.45565	-4.23876
C	8.42988	5.72192	-0.43971	H	-7.06777	10.25497	-2.55793
C	10.83942	4.34441	-0.51092	H	-11.06953	5.16583	2.48028
C	9.22912	5.80111	-1.56491	H	-10.34543	3.66614	-1.47771
C	8.83403	4.94999	0.66097	H	-11.78111	3.80628	0.54213
C	10.03376	4.26401	0.62656	H	-8.91577	6.39774	2.41633
C	10.44020	5.10716	-1.59834	H	-11.06953	-5.16583	-2.48028
C	7.64828	6.45869	2.15438	H	-10.34543	-3.66614	1.47771
C	7.23114	9.18857	2.44212	H	-8.91577	-6.39774	-2.41633
C	7.24397	7.23053	1.05367	H	-11.78111	-3.80628	-0.54213
C	7.84144	7.05316	3.38744	H	-7.77977	-8.89587	4.49619
C	7.63060	8.42604	3.52959	H	-6.72292	-9.18637	0.34442
C	7.03643	8.58988	1.19588	H	-7.06777	-10.25497	2.55793
C	-7.24397	7.23053	-1.05367	H	-8.15342	-6.45565	4.23876